Acid-Dependent Electrophilicity of Cyclopropylpyrroloindoles. Nature's Masking Strategy for a Potent DNA Alkylator

M. A. Warpehoski* and D. E. Harper

Contribution from Medicinal Chemistry, Upjohn Laboratories, Kalamazoo, Michigan 49001

Received March 24, 1994®

Abstract: Pseudo-first-order rate constants were determined for the solvolysis of adozelesin (**2**) and of several related cyclopropylpyrroloindoles (CPIs) as a function of pH and buffer concentration in mixed organic–aqueous solvents. Rate constants were proportional to the hydronium ion concentration at pH > 2, and the slope of the log k_{obs} vs pH plot was −1. Both the pyrrolidinoindole (**2a**) and piperidinoindole (**2b**) alcohols (ca. 4:1) were produced upon acid-catalyzed solvolysis of **2**. The products and kinetic behavior are consistent with rate-determining solvent attack on the protonated CPI and competing carbocation rearrangement. Reaction of **2** with HCl afforded predominantly the pyrrolidinoindole chloride **2e**, with only a trace amount (<5%) of the piperidinoindole chloride **2f**. Pseudo-first-order rate constants were proportional to both chloride and hydronium ion concentration. The products and kinetic behavior are consistent with attack of chloride ion on the protonated CPI. Comparison to the reported reactivity of spiro-[2.5]octa-1,4-dien-3-one (**6**) and bis(trifluoromethyl) quinone methide **8** suggests that the conjugated cyclopropyl ring of the CPI imparts a strong acid dependence to its reactivity with nucleophiles. This property may be relevant to the exceptional reactivity of the parent CPI antibiotic, CC-1065, toward duplex DNA.

Adozelesin (**2**, Scheme 1) is a potent antitumor agent presently in clinical trials.[1] It is a synthetic analog of CC-1065 (**1**), a highly toxic antibiotic isolated from *Streptomyces zelensis*.[2] The natural product[3] and synthetic analogs containing the 7b*R*,8a*S*-cyclopropylpyrroloindole (CPI) subunit[4] were shown to alkylate the N-3 atom of adenine in certain sequences of B form DNA, a reaction which appears to mediate the potent biological effects of these drugs.[5,6]

The CPIs differ from traditional chemotherapeutic alkylating agents, such as the nitrogen mustards and nitrosoureas,[7] in their pronounced selectivity for target nucleophilic sites in DNA[3,4] and their lack of reactivity with other biological nucleophiles.[5] Consistent with this selectivity, CPIs are remarkably chemically stable in neutral aqueous solutions.[8] CPIs have been reported to solvolyze under acidic conditions to give the cyclopropyl-ring-opened pyrroloindole alcohols or ethers (e.g., **2a** and **2c** in Scheme 1),[8,9] structures which are analogous to the cyclopropyl-ring-opened adducts formed in the reaction with DNA.[3,4]

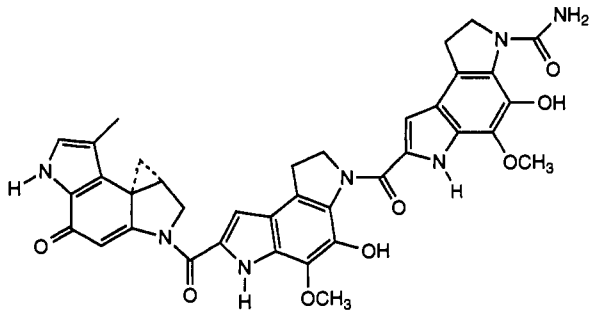

1

Experimental data on the chemical reactivity of CPIs are presently limited to qualitative information gained through synthetic experience[8,10] and to reported solvolytic half-lives for some CPIs[8] and altered alkylating drugs[11] in a single methanol/citrate buffer solution. As an initial step in understanding the unique DNA-selective reactivity of this unusual alkylating moiety, we studied the kinetics of the solvolysis and chloride ion reactions of adozelesin and several related CPIs (**2-5**, Scheme 1). These compounds were anticipated to have similar solvolytic properties, although they differed widely in solubility, DNA binding affinity, and biological potency.[4]

Experimental Section

Materials. Adozelesin (**2**), **3**, **4**, and **5** were synthesized at Upjohn Laboratories by previously reported procedures.[8,10a] Authentic samples of **2a**, **2e**, and **2f** were obtained by hydrogenolysis of the corresponding benzyl-protected phenolates. These, in turn, were intermediates (**2a** and **2e**) or minor by-products (**2f**) in the synthesis of **2**. Trichloroacetic acid (TCAH), tris(hydroxymethyl)aminomethane (tris), and inorganic salts

* Corresponding author. TEL 616-385-7389; FAX 616-385-5232.

® Abstract published in *Advance ACS Abstracts*, August 1, 1994.

(1) Li, L. H.; Kelly, R. C.; Warpehoski, M. A.; McGovren, J. P.; Gebhard, I.; DeKoning, T. F. *Invest. New Drugs* **1991**, *9*, 137–148.

(2) Hanka, L. J.; Dietz, A.; Gerpheide, S. A.; Kuentzel, S. L.; Martin, D. G. *J. Antibiot.* **1978**, *31*, 1211–1217. Martin, D. G.; Chidester, C. G.; Duchamp, D. J.; Mizsak, S. A. *Ibid.* **1980**, *33*, 902–903. Martin, D. G.; Biles, C.; Gerpheide, S. A.; Hanka, L. J.; Krueger, W. C.; McGovren, J. P.; Mizsak, S. A.; Neil, G. L.; Stewart, J. C.; Visser, J. *Ibid.* **1981**, *34*, 1119–1125. Chidester, C. G.; Krueger, W. C.; Mizsak, S. A.; Duchamp, D. J.; Martin, D. G. *J. Am. Chem. Soc.* **1981**, *103*, 7629–7635.

(3) Hurley, L. H.; Reynolds, V. L.; Swenson, D. H.; Petzold, G. L.; Scahill, T. A. *Science* **1984**, *226*, 843–844. Reynolds, V. L.; Molineux, I. J.; Kaplan, D. J.; Swenson, D. H.; Hurley, L. H. *Biochemistry* **1985**, *24*, 6228–6237.

(4) Hurley, L. H.; Lee, C.-S.; McGovren, J. P.; Warpehoski, M. A.; Mitchell, M. A.; Kelly, R. C.; Aristoff, P. A. *Biochemistry* **1988**, *27*, 3886–3892. Hurley, L. H.; Warpehoski, M. A.; Lee, C.-S.; McGovren, J. P.; Scahill, T. A.; Kelly, R. C.; Mitchell, M. A.; Wicnienski, N. A.; Gebhard, I.; Johnson, P. D.; Bradford, V. S. *J. Am. Chem. Soc.* **1990**, *112*, 4633–4649. Boger, D. L.; Coleman, R. S.; Invergo, B. J.; Sakya, S. M.; Ishizaki, T.; Munk, S. A.; Zarrinmayeh, H.; Kitos, P. A.; Thompson, S. C. *Ibid.* **1990**, *112*, 4623–4632.

(5) Li, L. H.; Swenson, D. H.; Schpok, S. L. F.; Kuentzel, S. L.; Dayton, B. D.; Krueger, W. C. *Cancer Res.* **1982**, *42*, 999–1004.

(6) Hurley, L. H.; Needham-VanDevanter, D. R.; Lee, C.-S. *Proc. Natl. Acad. Sci. U.S.A.* **1987**, *84*, 6412–6416. Weiland, K.; Dooley, T. P. *Biochemistry* **1991**, *30*, 7559–7565. Zsido, T. J.; Woynarowski, J. M.; Baker, R. M.; Gawron, L. S.; Beerman, T. A. *Ibid.* **1991**, *30*, 3733–3738. Sun, D.; Hurley, L. H. *Ibid.* **1992**, *31*, 2822–2829.

(7) Pratt, W. B.; Ruddon, R. W. *The Anticancer Drugs*; Oxford University Press: New York, 1979; pp 64–79.

(8) Warpehoski, M. A.; Gebhard, I.; Kelly, R. C.; Krueger, W. C.; Li, L. H.; McGovren, J. P.; Prairie, M. D.; Wicnienski, N.; Wierenga, W. *J. Med. Chem.* **1988**, *31*, 590–603.

(9) Martin, D. G.; Mizsak, S. A.; Krueger, W. C. *J. Antibiot.* **1985**, *38*, 746–752.

(10) (a) Kelly, R. C.; Gebhard, I.; Wicnienski, N.; Aristoff, P. A.; Johnson, P. D.; Martin, D. G. *J. Am. Chem. Soc.* **1987**, *109*, 6837–6838. (b) Boger, D. L.; Coleman, R. S. *Ibid.* **1988**, *110*, 4796–4807.

(11) Boger, D. L.; Ishizaki, T.; Kitos, P. A.; Suntornwat, O. *J. Org. Chem.* **1990**, *55*, 5823–5832.

0002-7863/94/1516-7573$04.50/0

Scheme 1

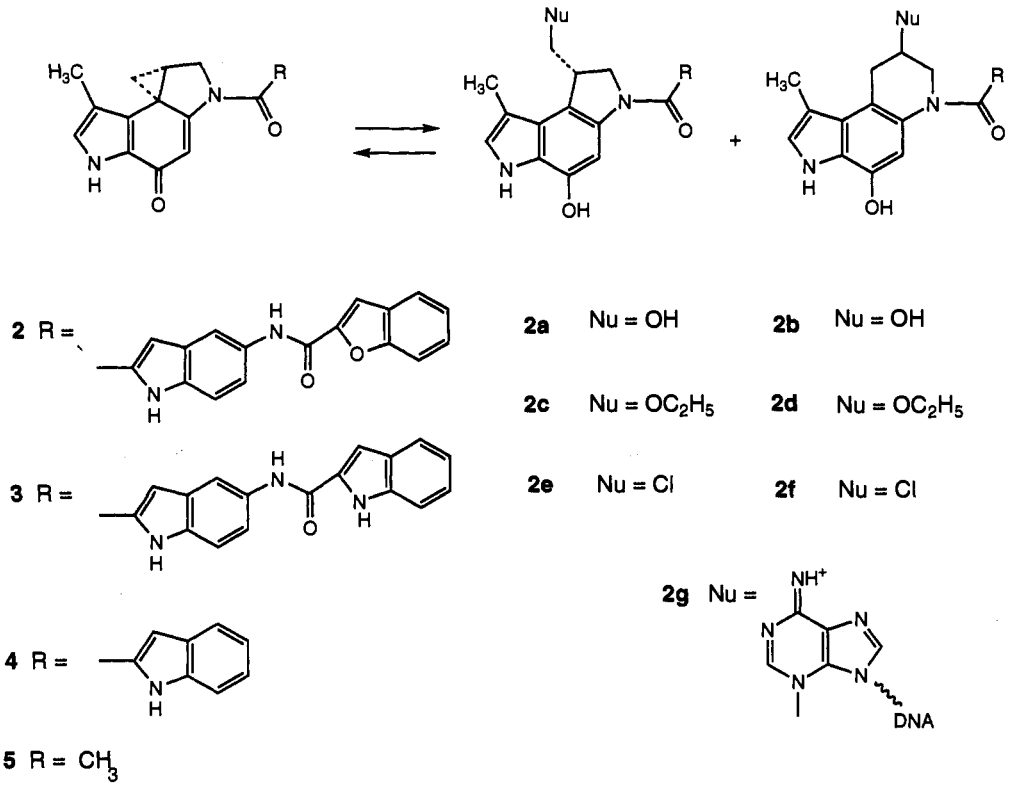

were of reagent grade and were used without further purification. For the kinetics studies, dimethylacetamide (Aldrich, 99+%), ethanol (AAPER, absolute), and water (McGaw, sterile for irrigation) were used as received. Trifluoroacetic acid-*d* (TFAD, Aldrich), DMSO-d_6 (Cambridge Isotope Lab.), DMF-d_7 (ICN), and D_2O (Stohler Isotope Chemicals) were used for NMR spectra. Preparative TLC was performed on Whatman PLKC-18F reversed phase (RP) plates developed in 75% methanol in water. TLC for densitometric analysis was carried out on either Whatman LKC-18D RP channeled plates developed in 75% methanol in water or Whatman LK6D silica gel channeled plates developed in 10% methanol in chloroform, 50% acetone in cyclohexane, or 40% acetone in methylene chloride. Densitometry (scanning at 300 nm) and UV spectra of TLC spots were run on a Shimadzu CS-930 scanning TLC densitometer. The pH measurements reported for the kinetic experiments were taken on the spent reaction mixtures using a Corning Model 255 ion analyzer equipped with an Orion Ross glass body, semimicro combination electrode. No corrections were made for the presence of organic solvents.

Products 3a and 3b. TCAH (0.08 mmol) in 0.7 mL of water was added to **3** (0.04 mmol) in 1.4 mL of DMSO and 0.5 mL of THF. After 3 h at 25 °C the mixture was poured into water and the yellow solid was filtered and dissolved in a small amount of acetone. Preparative TLC afforded two long-wavelength UV-quenching bands. The faster-moving band was eluted with acetonitrile to afford ca. 2 mg of **3b** as an off-white film (one spot, R_f = 0.4, on RP TLC, 70% methanol in water): ^{1}H NMR (DMF-d_7, 400 MHz) δ 11.77 (s, 1H, NH), 11.46 (s, 1H, NH), 10.68 (s, 1H, NH), 10.2 (s, 1H, amide NH), 8.28 (s, 1H, ArOH), 8.11 (s, 1H, ArH), 7.67 and 7.66 (overlapping d, 2H, distinguished by ^{1}H–^{13}C shift correlation), 7.58 (d, 1H), 7.49 (d, 1H), 7.47 (s, 1H), 7.24 (t, 1H), 7.08 (t, 1H), 7.06 (s, 1H), 6.43 (s, 1H), 6.38 (s, 1H), 4.26 (m, 1H, OCH), 4.24 (d, J = 10 Hz, 1H, NCH), 3.77 (m, 1H, N-CH), 3.63 (dd, J = 5, 16 Hz, 1H, OCCH), 3.13 (dd, J = 6.3, 16 Hz, 1H, OCCH), 2.49 (s, 3H, methyl); ^{13}C chemical shifts obtained from ^{1}H–^{13}C shift correlation δ 124.11, 123.75, 122.12, 120.23, 118.65, 112.74 (two carbons), 112.33 (eight of the ArCH), 106.16 (pyrrole CH), 104.47 (*o*-phenol CH), 103.66 (ArCH), 66.65 (OCH), 52.29 (NCH), 33.87 (CCH_2C), 12.76 (methyl); FAB HRMS M + H calcd for $C_{30}H_{26}N_5O_4$ 520.1985, found 520.1981; UV λ_{max} 314 nm (methanol); the sample exhibited negligible circular dichroism. In DMSO-d_6 solution the ^{1}H NMR spectrum of **3b** was very similar to that in DMF, except that the alcohol proton appeared as a doublet at δ 5.15 and the two high-field aromatic protons appeared as a singlet at δ 6.54; both of these signals disappeared when D_2O was added.

The slower-moving band afforded 8 mg of **3a** as a pale yellow solid (R_f = 0.3 on RP TLC, 70% methanol in water): ^{1}H NMR (DMSO-d_6, 300 MHz) δ 11.74 (s, 1H, NH), 11.63 (s, 1H, NH), 10.61 (s, 1H, NH), 10.18 (s, 1H, amide NH), 9.62 (s, 1H, ArOH), 8.20 (s, 1H ArH), 7.69–7.01 (10 H, ArH), 5.05 (t, 1H, OH), 4.62 (d, J = 10 Hz, 1H), 4.5 (dd, J = 9, 9 Hz, 1H), 3.69 (m, 2H), 3.15 (m, 1H), 2.36 (s, 3H, methyl); FAB HRMS M + D calcd for $C_{30}H_{25}N_5O_4$ + D 521.2047, found 521.2061; UV (methanol) λ_{max} 295 nm; circular dichroism (methanol) λ_{max} 270 and 318 nm, λ_{min} 295 nm. A solution of **3a** having an absorbance of 0.42 at 295 nm (1-cm cell) produced –4.3 millidegrees of ellipticity at that wavelength. In a separate experiment, perchloric acid (final concentration 0.02 M) was added to **3** (0.01 mmol) in 2.5 mL of THF, 0.5 mL of DMSO, and 0.6 mL of water. After 90 min the products were precipitated with water and filtered. RP TLC showed **3**, **3a**, and **3b**, in a ratio of 1:4:1 by densitometry at 300 nm. NMR (DMSO-d_6) showed the methyl signals of **3a** and **3b** in a ratio of ca. 6:1.

Addition of 5 μL of TFAD to 0.01 mmol of **3** in anhydrous DMSO-d_6 produced, within minutes, a major product whose aliphatic protons appeared at 4.67 (m, 1H), 4.57 (m, 2H), 4.37 (dd, 1H), and 4.06 (m, 1H). Signals possibly corresponding to a minor isomer were also detectable. Addition of 20% (v/v) D_2O to this solution slowly produced a mixture of **3a** and **3b**, in a ratio of 4:1. The same intermediates and final products were observed when D_2O was added prior to TFAD.

Products 2a and 2b. TFAD (20 μL) was added to 7 mg of **2** in DMSO-d_6 containing ca. 10% (v/v) of D_2O. The ^{1}H NMR spectrum (300 MHz) recorded after 1 h showed aliphatic proton signals at δ 4.7–4.5, 4.4, and 4.1 (ratio 3:1:1). After several hours the sample was precipitated with water and the yellow solid was separated. The ^{1}H NMR spectrum of this solid revealed two products, the major (4:1) product showing identical signals to those of an authentic sample of **2a**. The aliphatic signals of **2a** were indistinguishable from those of **3a** reported above. The minor product in the mixture showed aliphatic signals indistinguishable from those of **3b** reported above and was assigned the structure **2b**. RP TLC densitometric analysis at 300 nm of this mixture gave a ratio of **2a** to **2b** of 3:1. To examine the products formed under the conditions of the kinetics experiments, reaction mixtures at 5–40 times the drug concentration of the spectroscopic runs were prepared and analyzed by RP TLC. A solution of **2** (0.8 mM) in 50% (v/v) ethanol/water, containing 0.02 M tris-trichloroacetate (TTCA), final pH 2.1, showed loss of **2** over 90 min and the appearance of four major new peaks. The faster-moving pair (relative ratio 3:1 by densitometry) coeluted with **2a** and **2b**, respectively, obtained from the reaction described above. (These components also showed chromatographic properties identical to **2a** and

2b on silica gel.) The slower-moving pair of components were tentatively assigned as **2c** and **2d** (relative ratio 3:1 by densitometry). These products coeluted with the two major products formed in the reaction of **2** with TCAH in anhydrous ethanol. The UV spectra obtained from the TLC plates closely resembled those of **2a** and **2b**. The ratio of **2a** to **2c** and of **2b** to **2d** was slightly greater than 2:1, by densitometry. Several minor, very nonpolar components in the solvolysis reaction mixture were not characterized. Product analysis by TLC at early reaction times showed essentially the same product distribution as did the final mixture.

A solution of **2** (0.12 mM) in 50% (v/v) ethanol/water, containing 0.5 M TTCA, final pH 3.0, was allowed to react for 70 min, and the products were extracted with ethyl acetate. TLC on silica gel in two solvent systems showed no starting material, but only a minor spot corresponding to **2a**. The major spot was significantly less polar. A parallel reaction mixture containing 0.03 M TTCA and 0.5 M $NaClO_4$ showed mainly **2a** and unreacted **2** by TLC.

Products 2e and 2f. Addition of a small amount of HCl to **2** in DMF-d_7 afforded a sample of **2e**: ^{1}H NMR (300 MHz) δ 11.54 (s, 1H, NH), 10.86 (s, 1H, NH), 10.45 (s, 1H, amide NH), 9.3 (broad, OH), 8.37–7.1 (11H, ArH), 4.7 (m, 2H), 4.07 (m, 1H), 3.94 (dd, 1H), 3.62 (t, 1H), 2.42 (s, 3H, methyl). This spectrum was identical to that of authentic **2e**. A solution of **2** (0.8 mM) in 50% (v/v) ethanol/water, 0.02 M TTCA, final pH 2.1, containing 0.2 M NaCl, was analyzed after 10 min by TLC on silica gel. The preponderant (>95%) product coeluted with **2e** in three different solvent systems. Densitometry revealed a small, slightly less polar peak which had the same retention as an authentic sample of **2f**. The TLC spot of the minor product, upon standing in air, showed the same orange-red fluorescence under short-wavelength UV light as did authentic **2f**. This product was not isolated, however.

Kinetic Methods. Kinetic studies were conducted spectrophotometrically on a Beckman DU-70 scanning spectrophotometer, or, for the faster reactions, with a Beckman DU-7500 diode array instrument, with a thermostated cell compartment maintained at 25 ± 0.1 °C. Stock solutions of the CPIs (0.1–4 mg/mL) in ethanol or dimethylacetamide were added to 0.5 mL of the equilibrated ethanol/buffer mixtures and inverted to mix the sample. The reference blank contained all components except the drug. Spectra were scanned at 36 s or longer intervals (DU-70), or two wavelengths were monitored at shorter time intervals (DU-7500). The disappearance of **2** was generally monitored at 384 nm, that of **4** at 372 nm, and that of **5** at 354 nm, subtracting the absorbance at 650 or 470 as a background correction. Typically 90 data points, spanning at least three half-lives, were used to determine k_{obs}, although in some fast reactions fewer points were used, and in some slow reactions only one half-life was followed. Pseudo-first-order rate constants were obtained using a nonlinear curve fitting program adapted by F. J. Kezdy and K. D. Berndt. Graphic display (Grapher V1.77, Golden Software, Inc.) showed small (<1%) and fairly random residuals (Figure A, supplementary material). Rate constants were generally reproducible to within 5%, except for very fast reactions (half-life < 1 min), for which measurements varied within 15–20%. Second-order rate constants were calculated from the least-squares slope of linear plots of k_{obs} vs component concentration.

Results

Solvolysis Kinetics. Figure 1 illustrates the UV spectral change which accompanied the solvolysis of adozelesin (**2**) in 50% (v/v) ethanol/water containing 0.02 M tris-trichloroacetate (TTCA), at pH 2.2. The CPI peaks at 368 and 310 nm decayed to the absorbance of the cyclopropyl-ring-opened products. Sharp isosbestic points at 351, 328, and 303 nm indicated the absence of detectable intermediates. Spectral changes for the CPIs **4** and **5** were qualitatively similar, except that the solvolysis products of **5** showed no absorbance at wavelengths longer than 330 nm.

Absorbance decay of the long-wavelength band followed good first-order kinetics. Figure 2 shows the log plots of k_{obs} as a function of the measured pH for the solvolysis of **2** and **4** in the ethanol/water solvent mixture. Good linearity was observed over the pH range 2–3, with a slope of –1. The data for **2** and **4** were essentially identical. At pH values above 3, solutions of **2** in 50% (v/v) ethanol/water, 0.02 M TTCA, aggregated and precipitated at rates competitive with the greatly slowed solvolytic reaction. The more soluble **5**, however, could be studied in this pH range, and its observed solvolytic rate constant was close to that predicted from the linear portion of Figure 2. Under otherwise comparable

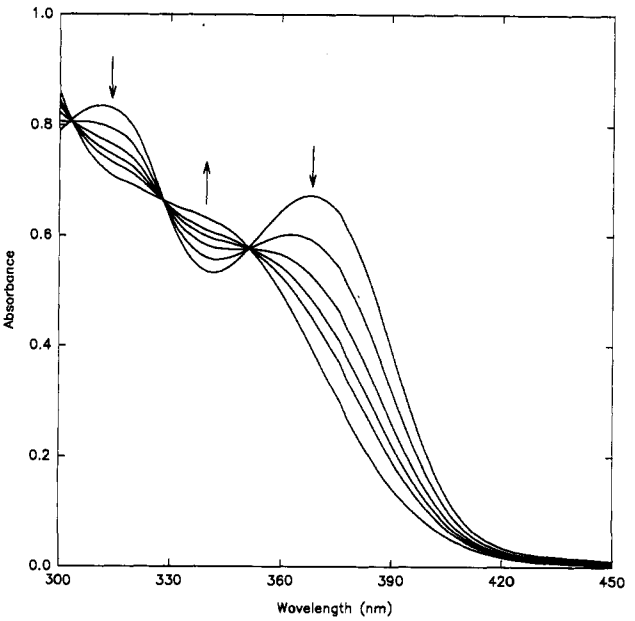

Figure 1. UV spectral changes during the hydrolysis of 20 μM **2** in 50% (v/v) ethanol/water containing 0.02 M TTCA, final pH 2.2, at 25 °C. The first five spectra were recorded at approximately 6 min intervals, and the last after 1 h.

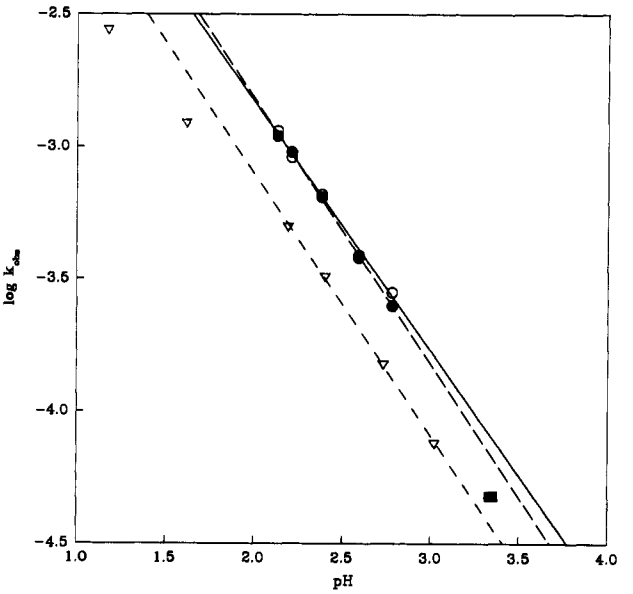

Figure 2. Logarithm of the observed first-order rate constants for the hydrolysis of 20 μM **2** (open circles), 30 μM **4** (solid circles), and 60 μM **5** (square) in 50% (v/v) ethanol/water, 0.02 M TTCA, at 25 °C as a function of measured pH. (In separate experiments in this buffer concentration and pH range, the addition of $NaClO_4$ up to 0.1 M had no effect on k_{obs}.) Log k_{obs} plotted vs pH for hydrolysis of 60 μM **5** (triangles) in 0.6% dimethylacetamide in aqueous buffer, 0.02–0.14 M TTCA, at 25 °C.

conditions, **5** underwent solvolysis only slightly more slowly than **2**, as observed previously.[8,12]

The hydrolysis of the more water-soluble analog **5** was also studied in aqueous buffer containing 0.6% dimethylacetamide. Linearity, also with a slope of –1, was found between pH 2 and 3, but negative deviation was apparent at lower pH values (Figure 2). At pH values below 1.5, the initially recorded spectrum showed a clearly discernible shoulder at 410–420 nm (A_{355}:A_{410} ca. 3:1),

(12) Rate constants (ref 8) for the solvolysis of racemic CPIs in a mixture of methanol and a pH 3 citrate buffer were in reasonable agreement with extrapolation of the present data. In the earlier work, the actual pH of the solvent mixture was not determined. We have prepared the solutions as described and measured a pH of 3.9.

Table 1. Effect of Buffer Concentration on k_{obs}

compound	solvent[a]	μ[b]	pH[c]	[TCA], M	$10^4 k_{obs}$, s^{-1}
2	ethanol/water	0.5	3.1	0.5	5.3
				0.3	2.9
				0.1	1.8
5	water[d]	0.3	2.7	0.07	1.2
				0.04	1.3
				0.02	1.2

[a] At 25 °C. [b] Maintained with $NaClO_4$. [c] Adjusted by addition of tris. [d] Contained 0.6% dimethylacetamide.

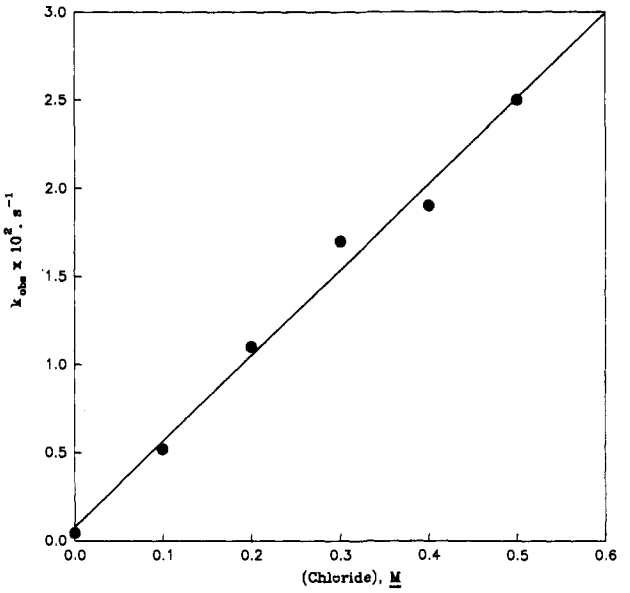

Figure 3. Dependence of the pseudo-first-order rate constant for the disappearance of 20 μM **2** on NaCl concentration in 50% (v/v) ethanol/water, 0.02 M TTCA, at pH 2.5, μ = 0.5 with $NaClO_4$, 25 °C.

presumed to originate from the protonated CPI. Rate constants for disappearance of this absorption were identical to those measured at the normal maximum.

The rate constants used in Figure 2 were obtained using dilute TTCA buffer solutions. While the observed rate constant for hydrolysis of **5** in 0.6% DMA in water was unaffected by TTCA concentration over the range 0.02–0.07 M, at high (0.1–0.5 M) TTCA concentrations, in the 50% (v/v) ethanol/aqueous buffer mixtures, observed rate constants for the disappearance of **2** increased with buffer concentration (Table 1).

Kinetics of Chloride Ion Reaction. The reaction of **2** with chloride ion in 50% (v/v) ethanol/acidic buffer solutions was much more rapid than its solvolysis at the same pH and cleanly generated **2e**, along with a very small amount (<5%) of **2f**. Figure 3 shows the linear relationship of the observed pseudo-first-order rate constant for the disappearance of **2** to the chloride ion concentration at constant pH and ionic strength in 50% (v/v) ethanol/water, 0.02 M TTCA. Dependence of k_{obs} at a fixed (0.2 M) chloride ion concentration on the hydronium ion concentration is presented in Figure 4. The relatively large error in measurement of these fast reaction rates by our technique, while minimally affecting the slope, does not provide an accurate determination of the intercept, i.e., the predicted k_{obs} at low hydronium ion concentration, from these data. Direct observation showed no evidence for chloride addition to **2** in neutral aqueous solutions. The UV spectrum of **2** (20 μM) in 50% (v/v) ethanol/water, 0.02 M TTCA, pH 7.0, 0.2 M NaCl, at 25 °C, showed a slight (<2%) decrease in absorbance over a period of 3 h. No isosbestic points could be discerned, however, and the small absorbance change under these conditions was attributed to slow drug aggregation.

The addition of hydrogen chloride to **2** at low pH in the ethanol/water solvent mixture went to completion under all conditions

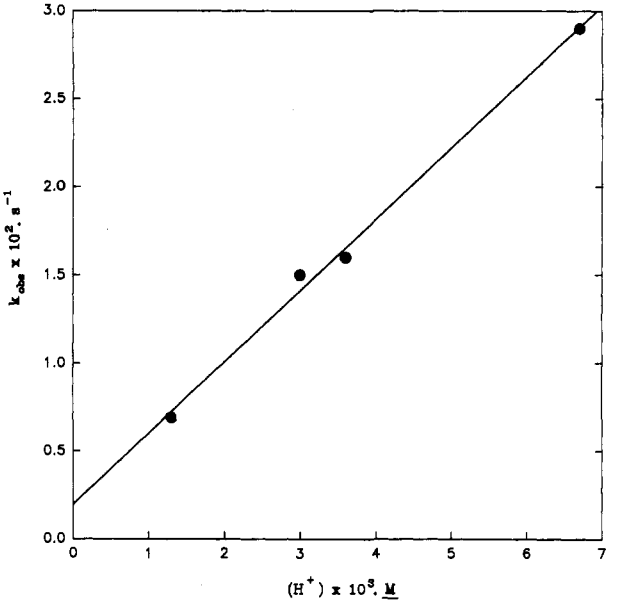

Figure 4. Dependence of the pseudo-first-order rate constant for the reaction of 20 μM **2** with 0.2 M NaCl on hydronium ion concentration in 50% (v/v) ethanol/water, 0.02 M TTCA, μ = 0.22, 25 °C.

described above. In 0.6% dimethylacetamide in aqueous buffer, however, **5** appeared to reach an equilibrium with its hydrogen chloride addition products in the presence of 0.1–0.5 M NaCl at pH 3 (data not shown). The decrease in absorbance of the CPI did not follow first-order kinetics. The net rate of ring-opening was significantly slower, however, than in the reaction of **2** with chloride ion in the ethanol/water solvent mixture. Competing hydrolysis of **5** under the reaction conditions stymied efforts to characterize the equilibrium.

Products. Previous product analyses, based on silica gel TLC and mass spectral evidence, had led us to presume that the CPI solvolysis products in aqueous acidic solutions were exclusively the pyrrolidinoindole structures (e.g., **2a** and **2c**, Scheme 1).[8] We have now shown that on RP TLC faster moving (more polar) components separated from both the alcohol and ether products. Preparative hydrolysis of **3**[13] allowed unambiguous identification of both the major product, **3a**, and the minor piperidinoindole isomer **3b** (Scheme 1). The structure of **3b** was established by heteronuclear chemical shift correlation. There was a single proton (δ 4.26) on the hydroxyl-bearing aliphatic carbon (δ 66.65), and the methylene group appeared at higher field. An unusual feature of the ^{1}H NMR spectrum of **3b** was the large upfield shift, to δ 6.4, of the two aryl protons on the piperidinoindole moiety. Further, these protons readily exchanged in the presence of D_2O, indicating rapid enolization through the adjacent heteroatom bond. Compound **3b** had lost almost all optical activity.

NMR revealed initial rapid cyclopropyl ring-opening of **3** in the presence of TFAD in >80% (v/v) DMSO-d_6/D_2O, but not to form **3a** and **3b**. The strongly downfield-shifted aliphatic signals suggested that TFA addition had occurred. Over a period of hours, **3a** and **3b** were formed, in a ratio of 4:1 (methyl signal integration). Hydrolysis of **3** in the presence of perchloric acid in a mixture of DMSO, THF, and water produced **3a** and **3b** in a ratio (NMR) of about 6:1. This similarity in product ratio suggested that the TFA reaction was a competing equilibrium and not an intermediate step in the hydrolysis.

Hydrolysis of **2** under the conditions of the NMR experiment produced an analogous initial and final product mixture. The ratio of **2a** to **2b** was also 4:1 by integration of the methyl signals. Densitometry at 300 nm of the RP TLC chromatogram showed

(13) Compound **3** was available in greater supply than the other CPIs, although its poor solubility precluded its use in kinetic studies.

Scheme 2

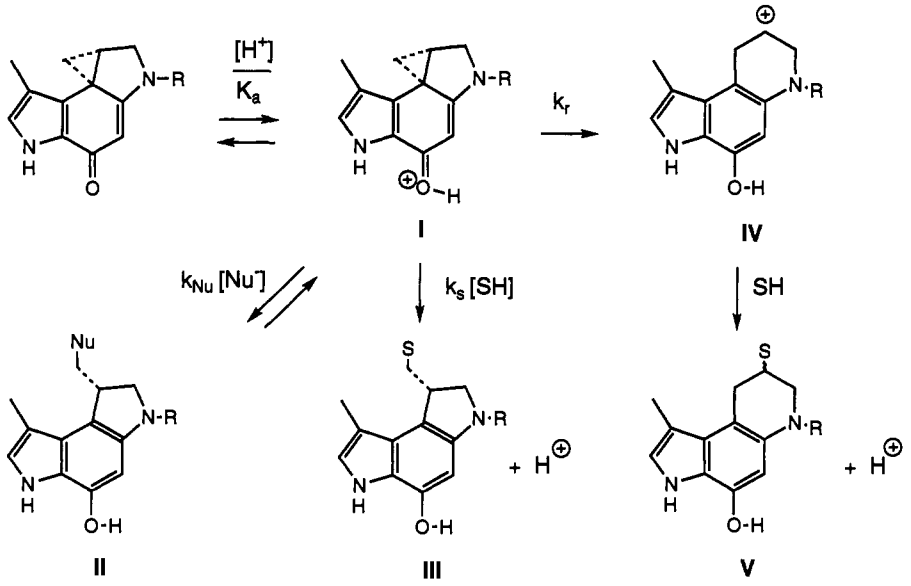

a ratio of 3:1, reflecting differences in extinction coefficients at this wavelength. TLC analysis of the solvolysis products of **2** under conditions similar to those of the aqueous ethanol kinetic runs showed that in dilute TTCA (0.02 M) the major products were **2a** and **2b** and another pair of products presumed to result from ethanol addition (**2c** and **2d**, Scheme 1). The approximate relative ratios (**2a**:**2b**:**2c**:**2d** ca. 6:2:3:1 by densitometry) did not vary with reaction progress. The ether products were stable under the reaction conditions and were produced in a similar relative ratio when **2** was reacted with TCAH in ethanol. However, reaction of **2** in the presence of 0.5 M TTCA (Table 1) gave a major initial product much less polar than **2a** on silica gel TLC. Unlike **2a**, this product did not give a well-defined spot on RP TLC. In conjunction with the NMR observations described above, it is proposed that this is the product of acid-catalyzed addition of TCA to **2**.

In contrast to the multiple products of the solvolytic reaction, chloride addition to **2** in acidic ethanol/water mixtures, or hydrogen chloride addition to **2** in DMF (NMR), gave predominantly **2e**. TLC analysis on normal-phase silica gel showed only a small amount (<5%) of a faster-moving component tentatively identified as **2f** on the basis of its chromatographic identity to an authentic sample.

Discussion

The simplest mechanism consistent with our data is shown in Scheme 2. In this mechanism, equilibrium protonation of the CPI generates the reactive electrophile **I**. Rate-determining addition of nucleophiles or solvent preferentially occurs at the least substituted cyclopropyl carbon to afford optically active pyrroloindole products **II** or **III**. In the slower solvolytic reaction, competing rearrangement to a secondary homobenzylic carbocation (**IV**), which is rapidly captured by solvent, occurs, giving racemic piperidinoindoles **V**. The expression for the observed solvolytic rate constant predicted from this kinetic model is given by eq 1, where $k_a = k_r + k_s[SH]$.

$$k_{obs} = k_a[H^+]/(K_a + [H^+]) \qquad (1)$$

Nonlinear curve-fitting of the observed rate constants for the hydrolysis of **5** in water (Figure 2) to eq 1 gave a good fit, with parameters $K_a = 0.063$ ($pK_a = 1.2$) and $k_a = 0.005$ s^{-1}. (The assumption is made that the measured activities approximate hydronium ion concentrations.) A pK_a of 1.2 for **I** is unusually high relative to that of protonated ketones (−4 to −7) and amides (ca. −1).[14] However, Baird and Winstein estimated a pK_a of 2 for the conjugate acid (**6H**$^+$) of spiro[2.5]octa-1,4-dien-3-one (**6**) in water, on the basis of the infrared carbonyl stretching frequency of **6** in CS_2.[15] Their estimate was supported by the exceptional basicity of the structurally similar 4-methylene-1,1,2,3,5,6-hexamethylcyclohexa-2,5-diene (**7**). The lack of a facile pathway for aromatization makes the conjugate acid **7H**$^+$ a surprisingly stable cation.[16]

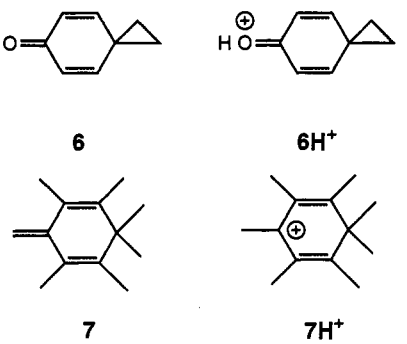

6 **6H**$^+$

7 **7H**$^+$

Interestingly, **7H**$^+$, in aqueous HCl solutions, has an absorbance maximum at ca. 400 nm ($\log \epsilon = 4$).[16] The conjugate acid of the unsubstituted CPI is relatively stable in aqueous acid and also shows an absorbance maximum around 400 nm (neutral solutions of this compound absorb at 360 nm).[8] The most reasonable site of protonation for this molecule is the conjugated carbonyl oxygen (Scheme 2, **I**, R = H), generating a species isoelectronic (in the six-membered ring) with **6H**$^+$ and **7H**$^+$. It has a pK_a in water of 2.7.[17] An *N*-acyl substituent on the CPI would be expected to lower its basicity. Thus, the kinetic data in Figure 2 give a reasonable estimate for the pK_a of **I** (Scheme 2, R = $COCH_3$). Consistent with this proposal for the structure of the conjugate acid of **5** was the observation of a significant shoulder absorbance at 410 nm in the initial spectra run at pH 1.2. These considerations lead us to favor Scheme 2, rather than a kinetically equivalent mechanism involving protonation at another functional group to give a nonreactive species.

With some assumptions, this mechanism can be extended to evaluate the data for the solvolysis of **2** and **4** in aqueous ethanol

(14) March, J. *Advanced Organic Chemistry: Reactions, Mechanisms, and Structure*, 2nd ed; McGraw-Hill: New York, 1977; pp 227, 228.
(15) Baird, R.; Winstein, S. *J. Am. Chem Soc.* **1963**, *85*, 567–578.
(16) von E. Doering, W.; Saunders, M.; Boyton, H. G.; Earhart, H. W.; Wadley, E. F.; Edwards, W. R.; Laber, G. *Tetrahedron* **1958**, *4*, 178–185.
(17) Harper, D. E. Unpublished.

Table 2. Rate Constants for Hydrolysis and HCl Reactions

compound	solvent	k_{H^+}, M^{-1} s^{-1} [a]	$10^4 k_0$, s^{-1} [b]	k_{HCl}, M^{-2} s^{-1} [c]
2	ethanol/water	0.15	NM[d]	20
4	ethanol/water	0.15		
5	water[e]	0.08		
8[f]	TFE/water	0.0032	0.17	0.44
6[g]	methanol	1 500 000	3.1	
9[h]	methanol		400	

[a] Slope of the linear plot of k_{obs} vs hydronium ion concentration (supplementary material, Figures B–D). $k_{H^+} = k_a/K_a$, where $k_a = k_r + k_s[SH]$ in the mechanism of Scheme 1. [b] Pseudo-first-order rate constant for uncatalyzed solvolysis. [c] Apparent third-order rate constant. [d] NM = not measurable. [e] Contained 0.6% of dimethylacetamide. [f] From ref 22. TFE = trifluoroethanol. [g] From ref 15. [h] From ref 23.

(Figure 2). First, it seems reasonable that the pK_a of **I** would be minimally affected by the nature of the *N*-acyl substituent. Secondly, since **I** is a charged species, its pK_a in 50% (v/v) ethanol/water is not likely to be significantly higher than in water.[18] Thus, 1.2 remains a reasonable estimate for the pK_a of the conjugate acids of **2** and **4** in aqueous ethanol. At $[H^+] \ll K_a$, k_{obs} should be linearly related to $[H^+]$, with a slope corresponding to k_a/K_a. The experimentally determined slopes are given in Table 2. Assuming $K_a = 0.063$ M, an estimate of $k_a = 0.01$ s^{-1} is obtained for both **2** and **4** in 50% (v/v) ethanol/water. This is only slightly higher than k_a for **5** in water. Both neutral nucleophilic attack on **I** and carbocation generation from a charged species (**I** → **IV**, Scheme 2) would be expected to show a small increase in rate with a decrease in solvent polarity.[19]

The solvolysis products likewise support the mechanism in Scheme 2. While the product of CPI reaction with chloride ion is almost exclusively the pyrrolidinoindole (e.g., **2e**), a significant fraction of the solvolysis products are piperidinoindoles (e.g., **2b**, **2d**), which could result from rearrangement of **I** to **IV**. Consistent with the intermediacy of **IV** is the almost complete loss of optical activity in an isolated sample of **3b**. Retention of chirality in **3a** implies that **IV** does not rapidly revert to **I**. The proportion of products arising from **I** and **IV** varied only slightly under several sets of experimental conditions. Taking $k_a = k_r + k_s[SH] = 0.01$ s^{-1} for the solvolysis of **2** in 50% (v/v) ethanol/water, as indicated above, the 4:1 ratio of **III** to **V** permits an estimate for k_r of 2×10^{-3} s^{-1}, and, for k_s, 2×10^{-4} M^{-1} s^{-1}. The mole ratio of water to ethanol in 50% (v/v) ethanol/water is about 3:1. We found a somewhat greater than 2:1 ratio (by densitometry at 300 nm) for alcohol/ether products for both **III** and **V**, indicating that **I**, like **IV**, shows little discrimination between these solvent nucleophiles.

The rapid equilibrium protonation postulated in Scheme 2 to account for the hydronium ion dependence of k_{obs} constitutes *specific* acid catalysis and predicts that k_{obs} should be independent of the concentration of acids weaker than the hydronium ion, such as buffer components. If, on the other hand, general acid-catalyzed pathways are important, the observed rate constant should follow eq 2, where k_{app} replaces the term k_a/K_a of eq 1, and k_{HA} is a second-order rate constant for the pathway catalyzed by the general acid HA.

$$k_{obs} = k_{app}[H^+] + \sum k_{HA}[HA] \qquad (2)$$

In aqueous TTCA buffer at pH 2.7, k_{obs} for the hydrolysis of **5** was unchanged over a buffer concentration range 0.02–0.07 M (Table 1). Other than the hydronium ion, TCAH is the strongest acid present. The pK_a of TCAH in water is 0.64;[20] thus, the fraction of TCAH in protonated form at equilibrium would be 0.01 at this pH. It is reasonable that a 10% increase in k_{obs} would be experimentally discernible. The absence of such an effect implies that k_{TCAH} must be less than 0.017 M^{-1} s^{-1}. Applying this maximum value for k_{TCAH} to the data in Figure 2 for the hydrolysis of **5** (in which the buffer concentration varied over the range 0.02–0.14 M) showed that *at most* 10% of the observed rate constant could be attributed to TCAH catalysis.

At much higher TTCA concentrations in aqueous ethanol the observed rate constants for disappearance of **2** did increase linearly with increasing buffer concentration (Table 1). However, TLC analysis of reaction mixtures run under these conditions indicated that the major product was not **2a**, but a much less polar material, presumably resulting from TCAH addition to **2**. The higher observed rate constants are thus not primarily due to general acid catalysis of solvolysis but to a competing bimolecular pathway. Consistent with this, addition of TFAD to DMSO-d_6 solutions of **2** or **3**, with or without a small amount of D_2O, had rapidly produced initial major products whose downfield-shifted aliphatic protons suggested TFA addition.

In a less polar environment than pure water, the negatively charged TFA and TCA ions evidently can act as nucleophiles with protonated CPI **I** (Scheme 2). The observed rate constants for disappearance of CPI under these conditions can be expressed by eq 3.

$$k_{obs} = (k_a/K_a)[H^+] + (k_{Nu}/K_a)[H^+][Nu^-] \qquad (3)$$

The slope of a plot of k_{obs} vs $[TCA^-]$ for the data in Table 1 is 8×10^{-4} M^{-1} s^{-1}. Dividing by the $[H^+]$ gives an apparent third-order rate constant, k_{Nu}/K_a, of about 1 $M^{-2}s^{-1}$. The numbers indicate that, even at TTCA buffer concentrations as low as 0.02 M, this bimolecular pathway contributed about 10–12% to the observed rate constants in 50% (v/v) ethanol/water (Figure 2). Thus, the corrected value for k_a in this medium is 0.009 s^{-1}. The small percentage of uncharacterized, nonpolar products from the solvolysis of **2** (Experimental Section) may have arisen from this TCA pathway.

No evidence for non-acid-catalyzed solvolytic (or TCA) cyclopropyl-ring-opening reactions could be observed. While the aqueous insolubility of CPIs precluded direct measurement of the solvolytic rate constant at pH values approaching neutrality, extrapolation of the linear region of Figure 2 to pH 7 provided an estimate of the half-life for a CPI under these conditions of greater than a year! The requirement for CPI protonation indicated in the mechanism of Scheme 2 is consistent with the observed stability under neutral conditions.

The reaction of CPIs with chloride ion in aqueous acidic solutions is also accommodated in Scheme 2, **I** → **II** (although we have no direct evidence ruling out a "concerted" pathway from the neutral CPI, in which the CPI, in the transition state, would have substantial cationic character). At pH values well above the pK_a of 1.2, and under conditions of sufficient chloride concentration, such that chloride addition products greatly predominate over solvolytic products, and the reverse reaction (**II** → **I**) is negligible, the observed rate constant is expressed by eq 4.

$$k_{obs} = (k_{Cl}/K_a)[H^+][Cl^-] \qquad (4)$$

These conditions appear to be met in the chloride reactions of **2** in aqueous ethanol summarized in Figures 3 and 4, which show the linear dependence of the observed pseudo-first-order rate constant on $[Cl^-]$ and $[H^+]$, respectively. Dividing the slope in Figure 3 ($\mu = 0.5$) by the constant hydronium ion concentration (0.05 M^{-1} $s^{-1}/0.0032$ M) gives an estimate of $k_{Cl}/K_a = 16$ M^{-2} s^{-1}. Dividing the slope in Figure 4 ($\mu = 0.22$) by the constant chloride concentration produces a comparable result (4 M^{-1} s^{-1}/

(18) Laitinen, H. A.; Harris,W. E. *Chemical Analysis*, 2nd ed.; McGraw-Hill: New York, 1975; pp 84–85.
(19) Ingold, C. K. *Structure and Mechanism in Organic Chemistry*, 2nd ed.; Cornell University Press: Ithaca, NY, 1969; pp 457–463.
(20) *Lange's Handbook of Chemistry*, 12th ed.; Dean, J. A., Ed.; McGraw-Hill: New York, 1979; p 5-40.

0.2 M = 20 M^{-2} s^{-1}), roughly 20-fold greater than the corresponding rate constant for TCA addition.

Bimolecular nucleophilic attack by chloride ion should be favored at the less substituted methylene carbon of the cyclopropyl ring of **I** (Scheme 2), consistent with product analysis (**2e**:**2f** > 95:5). If the small amount of piperidinoindole **2f** arises from direct chloride attack on the more substituted cyclopropyl carbon of **I**, it should retain chirality.[21]

While solvolysis of **5** was only slightly retarded in water, the addition of chloride ion in aqueous acid was drastically slowed. This solvent response is expected for bimolecular reaction of an anion and a cation (Cl^- and **I**, Scheme 2).[19] Retardation of this reaction resulted in complex kinetic behavior, including reversal (**II** → **I**) and solvolysis.

There are some interesting contrasts in the reactivity of CPIs relative to that of quinone methides such as **8**.[22] Most notably, **8** readily reacted with nucleophiles in the absence of acid catalysis. In neutral aqueous trifluoroethanol, **8** had a half-life of only 11 h. Furthermore, it reacted with chloride ion in a non-hydronium-ion-dependent reaction. The second-order rate constant reported for this reaction, 0.02 M^{-1} s^{-1}, would give an observed pseudo-first-order rate constant of 0.004 s^{-1} at 0.2 M chloride ion, at neutral pH, i.e., a half-life of about 3 min. In contrast, under comparable conditions in ethanol/water solution, **2** showed no evidence of chloride addition in 3 h (its instability with respect to aggregation and precipitation precluded further measurement).

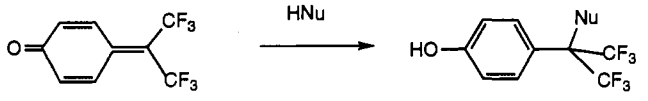

8 Nu = OH, Cl

Despite its greater electrophilicity under neutral conditions, **8** was nearly 50-fold *less* reactive to both hydronium-ion-catalyzed solvolysis and chloride addition than was CPI **2** (compare k_{H^+} and k_{HCl} in Table 2). This low reactivity is consistent with the low pK_a (estimated −8.1)[19] of its conjugate acid. Even at pH 3, solvolysis of **8** occurred predominantly by the non-hydronium-ion-catalyzed pathway.

The reactivity of the labile spiro[2.5]octa-1,4-dien-3-one (**6**) suggests that the conjugated cyclopropyl ring strongly influences reactivity patterns. Baird and Winstein first generated **6** in situ and showed that it underwent cyclopropyl ring-opening under both acidic and basic conditions.[15] It was, however, especially sensitive to acid, with a second-order methanolysis rate constant in excess of 10^6 M^{-1} s^{-1} in methanol (Table 2). Thus, even at "pH" (−log($CH_3OH_2^+$)) values approaching 10, the acid-catalyzed pathway predominated over the "uncatalyzed" and methoxide catalyzed pathways.

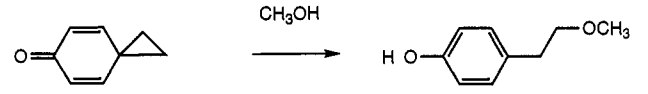

6

Baird and Winstein noted that the cyclopropane ring in **6** must be orthogonal to the plane of the cyclohexadienone ring, effectively extending its conjugation. The UV spectrum of **6** in methanol was remarkably similar to that of quinone methide **9**. But while **9** had a half-life of only 17 s in methanol at 25 °C, the half-life of **6** was about 40 min (from k_0, Table 2).[15,23] Thus, homologation of the quinone methide via the cyclopropane retained its electronic conjugation, but significantly enhanced its stability in a nucleophilic solvent. Both the CPIs and "cyclopropyl quinone methide" **6** thus appear to show a greatly diminished intrinsic electrophilicity relative to their classically unsaturated counterparts. Their reactivity as electrophiles is profoundly acid-dependent.

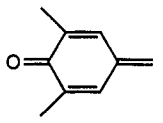

9

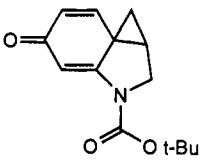

10

The greatly reduced reactivity to both acid-catalyzed and uncatalyzed solvolysis of the CPI structure relative to **6** (Table 2) must reflect the influence of the flanking nitrogen heterocycles. The conjugated methylpyrrole ring might be expected to contribute most significantly to that stabilization. This is consistent with the report by Boger et al. that N-BOC-CI (**10**) has a half-life of only about 5 h in 50% (v/v) methanol/water at neutral pH.[24]

Finally, we note some interesting phenomenological parallels in the observed kinetic behavior of the hydrolysis of CPIs (an acid-catalyzed addition reaction) and of the hydrolysis of mitomycins (an acid-catalyzed elimination reaction) reported by McClelland and Lam.[25] The mitomycin hydrolysis is multistep, with its rate-determining step being the acid-catalyzed elimination of a methanol molecule. Subsequent formation of the quinone methide and its reaction with water are extremely fast in comparison. Nevertheless, above pH 3 mitomycin C hydrolyzed with a pseudo-first-order rate constant which was linearly dependent on the hydronium ion concentration, with a slope of nearly −1 for the log k_{obs} vs pH plot. The second-order hydrolysis rate constant was only 8-fold greater than that which we determined for **2**. At pH values below 3, protonation at nitrogen atoms in the drug caused a leveling of the observed rate constants. Extrapolation of the reported data to pH 7 gave an estimate of the half-life for mitomycin C in water at 25 °C of approximately 3 months, approaching that estimated for CPIs. In vivo, the reaction of mitomycin with DNA is even more complex, because it is bioreductively activated.[26] However, unreduced mitomycin C does alkylate DNA in vitro at pH 4.[27] Structurally simpler analogs of mitomycin, which do not require bioreductive activation, have shown mitomycin-like sequence recognition in their alkylation of DNA.[28]

It is intriguing that both of these structurally complex, DNA-targeted, natural product alkylating entities (CPI and mitomycin) are potentially activated by comparably acidic environments, through chemically different mechanisms.[29] Computations by Lamm and Pack have highlighted the intrinsically high acidity associated with the grooves of duplex DNA, a consequence of its ordered, polyelectrolyte nature.[30] These authors suggested that

(21) Although **2f** was not isolated from this reaction, it is noteworthy that the authentic sample of **2f** was optically active. In this case the rearrangement (during mesylate displacement) occurred in the benzyl-protected phenolate.

(22) Richard, J. P. *J. Am. Chem. Soc.* **1991**, *113*, 4588–4595.

(23) Filar, L. J.; Winstein, S. *Tetrahedron Lett.* **1960**, (25), 9–16.

(24) Boger, D. L.; Wysocki, R. J., Jr.; Ishizaki, T. *J. Am. Chem. Soc.* **1990**, *112*, 5230–5240.

(25) McClelland, R. A.; Lam, K. *J. Am. Chem. Soc.* **1985**, *107*, 5182–5186.

(26) Szybalski, W.; Iyer, V. N. *Fed. Proc.* **1964**, *23*, 946.

(27) Tomasz, M.; Lipman, R.; Lee, M. S.; Verdine, G. L.; Nakanishi, K. *Biochemistry* **1987**, *26*, 2010–2027.

(28) Weidner, M. F.; Sigurdsson, S. T.; Hopkins, P. B. *Biochemistry* **1990**, *29*, 9225–9233.

(29) The potential "common chemical basis" between the acid-catalyzed solvolytic behavior of anthramycin and activation of its alkylation by DNA has also been proposed: Kohn, K. W.; Glaubiger, D.; Spears, C. L. *Biochim. Biophys. Acta* **1974**, *361*, 288–302.

(30) Lamm, G.; Pack, G. R. *Proc. Natl. Acad. Sci. U.S.A.* **1990**, *87*, 9033–9036.

this property of DNA is responsible for the observed[31] activation, by DNA, of polycyclic aromatic diol epoxides, including some potent carcinogens. If the acidic environment associated with DNA can influence the reactivity, and hence the biological consequences of adventitious carcinogens, it seems reasonable to speculate that nature would exploit this same property in the evolution of antibiotics that target DNA as an initial step in their biological action.[32]

Acknowledgment. We thank Ilse Gebhard and Paul D. Johnson for synthesizing the CPIs used in this study and for providing authentic samples of **2a**, **2e**, and **2f**, and we thank Steve Mizsak for conducting the HETCOR NMR analysis of **3b**.

Supplementary Material Available: The first-order decay curve and residuals for Figure 1, plots of k_{obs} vs $[H^+]$ for Figure 2, and UV spectral changes for **2** at pH 7 (5 pages). This material is contained in many libraries on microfiche, immediately follows this article in the microfilm version of the journal, and can be ordered from the ACS; see any current masthead page for ordering information.

(31) Geacintov, N. E.; Ibanez, V.; Gagliano, A. G.; Yoshida, H.; Harvey, R. G. *Biochem. Biophys. Res. Commun.* **1980**, *92*, 1335–1342. Michaud, D. P.; Gupta, S. C.; Whalen, D. L.; Sayer, J. M.; Jerina, D. M. *Chem.-Biol. Interactions* **1983**, *44*, 41–52.

(32) Williams, D. H.; Stone, M. J.; Hauck, P. R.; Rahman, S. K. *J. Nat. Prod.* **1989**, *52*, 1189–1208.